The Thesis Committee for Bryant Timothy Kopriva
Certifies that this is the approved version of the following thesis:

Response of Minibasin Subsidence to Variable Deposition: Experiments and Theory

APPROVED BY
SUPERVISING COMMITTEE:

Supervisor:

Wonsuck Kim, Supervisor

James Buttles

Charles Kerans

Response of Minibasin Subsidence to Variable Deposition: Experiments and Theory

by

Bryant Timothy Kopriva, B.S. Geo. Sci.

Thesis

Presented to the Faculty of the Graduate School of

The University of Texas at Austin

in Partial Fulfillment

of the Requirements

for the Degree of

Master of Science in Geological Sciences

The University of Texas at Austin

May 2012

Dedication

To my mother for pushing me into a career in the earth sciences, and my brother for his companionship over the past years.

Acknowledgements

I would first like to thank my advisor Wonsuck for believing in me and making sure that I made it in to graduate school in the first place. Without his excellent coaching I would have never been able to accomplish what I have. I would like to thank Jim for introducing me to experimental geology and giving me the opportunity to work on many different projects. Charlie my last committee member has been an excellent instructor and has taught me a large portion of any geologic knowledge that I might have, both in the classroom and the field. I would like to thank a few people that have contributed insight to this work, Luc Lavier for his support with programming questions, Wynn Kopriva for advice on engineering matters, and Kiran Sathaye for his help with modeling approaches. Philip Guerrero, the graduate school coordinator of the graduate school has helped a great deal in making my progress through the program smooth and trouble free, and I can say he has truly become a close friend over these past years. I would finally like to thank all of my friends that I have become close to here in Austin as it our relationships that have shaped me into the person that I am today.

Abstract

Response of Minibasin Subsidence to Variable Deposition: Experiments and Theory

Bryant Timothy Kopriva, M.S. Geo. Sci.
The University of Texas at Austin, 2012

Supervisor: Wonsuck Kim

Differential loading induced deformation of a mobile substrate (e.g., salt tectonics) is an important process for the development of accommodation space and stratigraphic architectures in intra-slope minibasins. Numerous studies of minibasin systems have focused on either the tectonic processes involved in salt body deformation or the stratigraphic interpretation of the overburden sediment deposits. This study, however, focuses on coevolution of depositional and tectonic processes and provides a new insight of the linked evolution into the stratigraphic patterns. Using a silicone polymer to simulate a viscous mobile substrate, a series of 2D experiments were conducted to explore the effects of variation in 1) sedimentation rate, 2) depositional style (intermittent sediment supply), and 3) the thickness of the deformable salt substrate on subsidence patterns and minibasin evolution. Experiments results have shown that larger initial thickness of salt substrate as well as lower sedimentation rate caused greater

amounts of subsidence for a given amount of deposit. Furthermore, increase in subsidence rate was observed as sedimentation continued, while decrease in subsidence rate occurred once sedimentation ceased. Due to the linked depositional and tectonic processes, higher sediment supply resulted in relatively slower subsidence and more actively widening minibasins. Lower sediment supply was observed to have the reverse effect, resulting in higher relative subsidence and a narrow basin width. A numerical model that captures viscous flow under the deposit is also presented here. The model for minibasin formation showed the effects of interaction of the two processes (deposition and tectonics) on the development of minibasin strata in the experiments. Experimental and modeled findings have resulted in a new model of minibasin development that incorporates the effects of sedimentation rates on subsidence patterns into basin evolution.

Table of Contents

List of Tables

List of Figures

CHAPTER 1: INTRODUCTION AND PREVIOUS WORK

Introduction

Inter-slope minibasins, such as those found in the Gulf of Mexico, are "synkinematic basin[s] subsiding into relatively thick, allochthonous or autochthonous salt" (Jackson and Talbot, 1991). These small (< 10 km wide) basins are locations of rapid (up to 1 km/ma) subsidence of the overburden sediment into a ductile salt substrate (Hudec et al., 2009). These salt withdrawn basins often develop in association with significant hydrocarbon deposits (Weijermars et al., 1993). Successful hydrocarbon exploration within these systems is dependent on accurate interpretation of stratigraphy within the basins.

Two approaches have often been taken when studying minibasin systems. A salt-tectonic approach has focused on the structural aspects such that deformation of a mobile salt body drives stratal development. Studies by Jackson and Vendeville (1994), Vendeville and Jackson (1991a and 1991b), and others explored the behavior of a mobile salt under a variety of tectonic conditions, i.e. extensional or compressional tectonic regimes, to understand large-scale change in basin accommodation. Contrastingly, a depositional history approach has focused on the changes in sedimentary processes within minibasins and the stratigraphy that develops as a result of the changes. Studies by Prather et al. (1998), Winker and Booth (2000), and others have developed dynamic depositional models based on the observed stratigraphy and attempted to link sediment transport to minibasin strata. While understanding of these end-member systems is a necessary step for interpreting subsurface geology, a unified understanding of the linked two processes is also required.

This study attempts to better understand the tectonic (subsidence) response to changing sedimentary conditions and the subsequent stratigraphic development, using a series of process analogue experiments under precisely controlled boundary conditions and theoretical model that captures the experimental results. We also briefly discuss the application of our experimental and modeling results to the minibasin stratal development in natural scale.

Subsidence mechanism overview

A variety of different processes may contribute to the subsidence mechanisms in salt withdrawn minibasins (Hudec et al., 2009). Subsidence may be driven by 1) buoyancy forces, i.e. a dense sedimentary deposit floating upon a less dense mobile salt (Hudec et al., 2009), 2) tectonic forces, such as diaper shortening (Humphris 1978; 1979), extension related diaper fall (Vendeville and Jackson, 1992a), subsalt deformation and faulting (Vendeville et al., 1995; Schultz-Ela and Jackson, 1996), downhill flow of salt sheets causing decay of salt topography (Talbot, 1998), or by 3) differential sediment loading on the mobile salt (Talbot, 1986). Prevalence of one of these mechanisms of subsidence is determined by tectonic environment, slope gradient, sedimentation rate, and salt geometry. These factors can vary from region to region creating a wide range of minibasin styles (Hudec et al., 2009). Hudec et al. (2009) has shown that buoyancy forces alone are insufficient to initiate minibasin formation due to the low initial density of clastic sediments, leaving tectonic subsidence and sediment loading as the viable methods of minibasin initiation. Tectonic regimes likely control the formation and geometries of minibasins but vary independently of sedimentary processes. Although subsidence in salt withdrawn

minibasins can be influenced by this variety of tectonic and gravity processes, previous studies have highlighted the importance of subsidence induced by a differential sediment load, especially on minibasin initiation (Weijermars et al., 1993; Cohen and Hardy 1996). Deformation resulting from differential loading results from sediments of laterally variable thickness causing lateral pressure differences on the substrate which induce flow in this mobile layer (Cohen and Hardy 1996). In this study we focus on the interaction between an increasing sedimentary load and the deformation of salt due to this differential stress field, as it provides a direct link between sedimentary and tectonic processes.

Salt Dynamics Overview

It is generally considered that salt behaves as a Newtonian fluid and has no effective yield strength even at very shallow burial depths (meters) (Weijermars et al., 1993). A Newtonian material responds instantaneously to an applied stress and displays a linear relationship between that stress and the resulting accommodated strain. This implies that a load applied to a mobile salt substrate would induce an instantaneous change in the subsidence profile. However, given the high viscosity of salt when compared to other Newtonian fluids it is possible that the deformation of the salt body is unable to respond instantaneously to a dynamically increasing sedimentary load. We hypothesize that sedimentary systems in which the sedimentation rate exceeds the response time of the highly viscous salt will exhibit a non-linear subsidence profile due to an increasing sediment load. This non-linear subsidence profile occurs independently of any allogenic forces on the system and can alter the stratigraphic relationships that develop. Considering differential sediment loading as an important subsidence mechanism for minibasin initiation and

subsidence patterns, understanding the dynamics of salt withdrawal under an imposed sedimentary load is fundamental to unraveling the stratigraphic relationships of the minibasin system.

CHAPTER 2: EXPERIMENTAL METHODOLOGY

Salt Analogue

Mobile substrate (salt) was model with a viscous silicone polymer, polydimethylsiloxane, often referenced by the Dow Corning, USA code SGM-36. SGM-36 has been extensively used to simulate salt in laboratory experiments due to its similar rheological behavior to salt (e.g. Vendeville and Jackson, 1992a; 1992b). Weijermars et al. (1986; 1993) has rigorously explained the application of the material to experimental models of natural salt in detail and thus we provide only a brief summary here. Under experimental sediment loading conditions this polymer behaves as a linear viscous fluid (Newtonian fluid). The viscosity of the material is low enough to deform over experimental time scales (hours) allowing simulation of salt deformation over basin filling time scales (thousands of years). These properties make SGM-36 useful to simulate the dynamics of wet salt which deforms by diffusion creep, the deformation of solids by diffusion of vacancies through the crystal lattice (Weijermars et al., 1993). Wet salt effectively has no yield strength over short geologic time scales, even at shallow burial depths, and can also be described as a viscous Newtonian material (Weijermars et al., 1993). A scaling analysis between experimental and natural systems is presented within the discussion.

Experimental Design

A series of 14 experiments (henceforth Exp. 1~14) were conducted in a 100 cm wide, 50 cm tall, and 10 cm deep clear polycarbonate flume. Experimental parameters are

listed in Table 1. Prior to the start of experiments silicone polymer was added to a specified depth within the flume and then allowed to flow flat under the influence of gravity. Using a computer controlled sediment feeder, quartz sand (D_{50} = 200 μm) with a density of 1200 kg/m^3 was point loaded into the center of the flume. This created an angle of repose sediment pile which induced a differential load on the polymer. The sedimentary deposit rested on and slowly subsided into the polymer. Polymer displaced by the subsiding sediments flowed outwards from below the sediment pile and upwelled close to the sides of the flume (Figure 1). Blue colored sand was added at 5 minute time intervals. This was an attempt to track the internal deformation of deposit. Distortion due to edge effects prevented clear observation of internal deformation. Orange beads within the polymer allowed observation of flow paths as the polymer substrate was displaced by subsiding sediments. The sediments and polymer were separated by a thin sheet of waxed paper to aid in experiment cleanup. One experiment run without waxed paper displayed no noticeable difference in overall subsidence patterns to other experiments showing that isostatic influences of the paper were insignificant to the subsidence patterns.

Sediment supply rates were held constant throughout each run but varied across the experiment suite. To explore the subsidence patterns under different loading conditions, three different sediment feed rates (i.e., low, medium, and high) were used to observe the subsidence patterns. These changes in feed rate were coupled with experimental runtime to keep the total amount of sediment added to the basin constant for each experiment. Constant total amount of sediment isolated the control of sedimentation rates on subsidence patterns.

Eight experimental runs were conducted utilizing a thin initial polymer substrate depth (η_{PI} = 8 cm). Eight equivalent experiments were tested with a thick initial substrate depth (η_{PI} = 16 cm) to indicate dependence on salt body thickness. The two thicknesses served as process analogue model for "confined" and "unconfined" natural basins. A thin polymer substrate represented a "confined" minibasin system while thicker substrate represented an "unconfined" minibasin arrangement. In this study a confined system was defined as a sediment-filled minibasin that is able to subside nearly to the point at which sediments contact the ridged basement and form a salt weld over the time period that the system is observed. An unconfined system was defined as a minibasin in which the sediments were not able to subside close (within 5 cm in the experiments) to the point of contact with the rigid basement over the time period which the system is observed. By utilizing two thicknesses of polymer in experiments the role of substrate thickness on subsidence patterns, as well as comparisons of edge effects in confined and unconfined systems were observed.

Sedimentation in deep water clastic systems such as those simulated by experiments is dominated by turbidity currents which are important mechanisms for the sediment transport from shallow water sources into deep water depositional sinks (Lamb et al., 2010). Turbidity currents can be generated by mass failures (Normark et al., 1993) and/or by other infrequent events such as hyperpycnal plumes (Lamb et al., 2010). Additionally Primez et al. (2012) has shown that periods of high sedimentation correspond to sea-level lowstand, while sedimentation rates were low during subsequent highstand. In order to capture the natural minibasin systems that receive sediment through these infrequent turbidity current

events, as well as cycles of sedimentation that correspond to 15-20 ka eustatic cycles, experiments were ran with periods of intermittent sedimentation. Intermittency was either zero, i.e. constant sedimentation, 5 minute cycles (5 minutes of sedimentation followed by 5 minutes of non-deposition), or 30 minute cycles. Two frequencies of sedimentation were designed to observe subsidence patterns resulting from material response to different periods of non-deposition, allowing for different periods of substrate response time for an equivalent sediment load. These infrequent sediment loads demonstrated how subsidence profiles respond to a pulse or cycle of sediment entering the basin.

EXP #	Runtime (hr)	Sed Feed Rate (cm^3/s)	Polymer Depth (cm)	Intermitency Frequency (min)
1	1:00	2	8	none
2	2:00	1	8	none
4	2:00	2	8	30
5	1:00	4	8	30
6	1:00	4	8	5
7	2:00	2	8	5
9	2:00	1	16	none
10	1:00	2	16	none
11	1:00	4	16	30
12	1:00	4	16	5
13	2:00	2	16	30
14	2:00	2	16	5

Table 1: Experimental runs conducted in this study. Six experiments were conducted with 8 cm of deformable polymer under sediment feed rates of 1, 2, and 4 cm^3/s, representing low, medium, and high rates of sediment supply respectively. These feed rates were coupled with experiment runtime to keep the total volume of sediment constant across all runs. Imposing intermittent sedimentation doubled runtime when compared to constant sedimentation experiments of the same feed rates. An additional suite of 6 experiments was conducted with equivalent sedimentary conditions with 16 cm of initial polymer substrate depth.

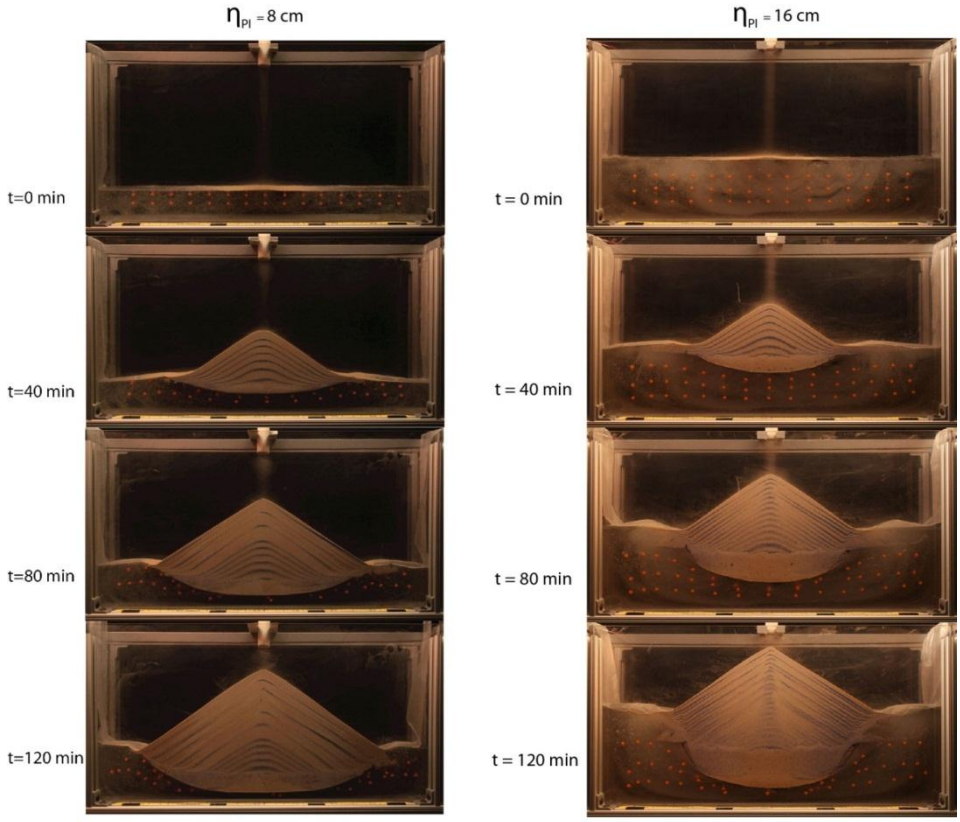

Figure 1: Sequence of digital images illustrating the progression of Exp. 2 and Exp. 10, with a constant low (1 cm^3/s) sedimentation rate throughout the two hour runtime. Experiment 2 (left sequence) had initial polymer thickness of 8 cm, while experiment 10 (right sequence) had initial polymer thickness of 16 cm. Notice the depth and width differences between the two created basins. Experimental flume measures 1 m wide, 0.5 m tall and is 0.1 m deep. As the polymer is loaded with sediment it is displaced by the differential load and upwells at the edges of the subsiding sediment pile.

Data Collection and Processing

For each run the evolution of the minibasin system was observed through the usage of time-lapse imagery. Images were taken automatically in 20-sec intervals throughout the experiment. Utilizing image-processing software the images were first corrected for lens distortion and perspective. Once the images had been corrected and properly scaled, MATLAB image processing codes developed specific to these experiments allowed for automated mapping of the top and bottom surfaces of the sediment pile for each image. The mapped surfaces provided values of subsidence, overburden thickness, basin width, as well as area of created accommodation (Figure 2).

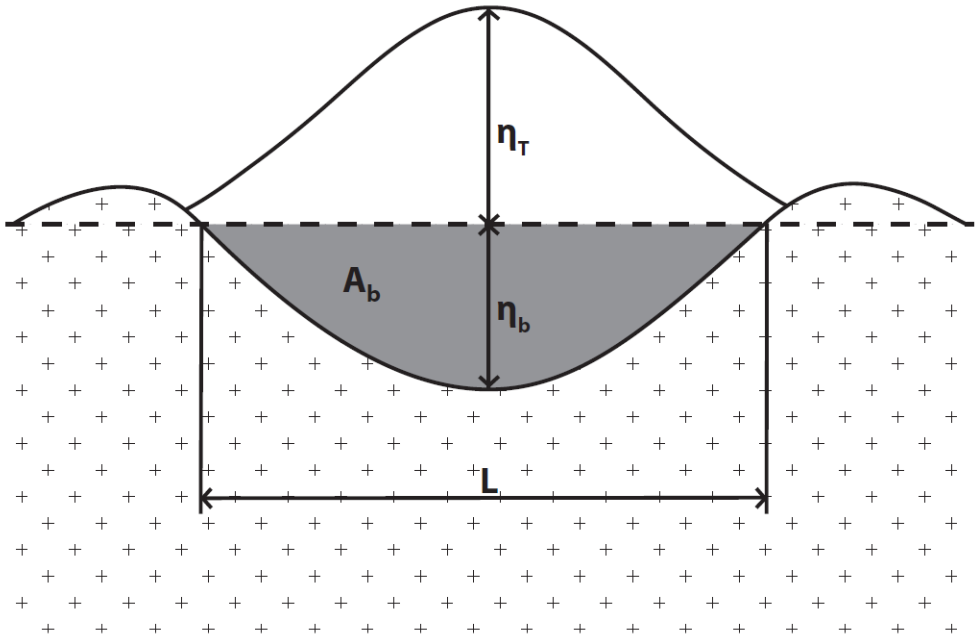

Figure 2: Schematic of data collected from each image. For each 20 second interval the top and bottom surfaces of the sediment deposit were mapped. From these mapped surfaces η_T the max sediment pile height, as well as (η_b) the maximum subsidence were recorded. Sediment pile heights as well as vertical subsidence were captured at 5 cm offset intervals laterally from the sediment pile centerline. Area of created accommodation space (A_b) (dark shaded region) as well as the width of the basin L were recorded from each image.

CHAPTER 3: EXPERIMENTAL RESULTS

Role of Substrate Thickness

Substrate thickness was one of the dominant controls in the total subsidence of the sedimentary deposit through the experimental run. Thicker initial substrate depths (η_{PI}) resulted in greater subsidence per time in each of the experimental cases (Note the scale change of the vertical axis between Figure 3A and 3B to Figure 4A and 4B). This unconfined basin setting, (i.e., Experiments with η_{PI} = 16 cm) yielded a much larger amount of subsidence. During the experiments with thick initial substrate (η_{PI} = 16 cm), overburden sediments did not approach close to the rigid basement by the end of experimental runs (Figure 4A and 4B). However, equivalent experiments with thin initial substrate thickness (η_{PI} = 8 cm) (Figure 3A and 3B) showed the sediment subsided near the rigid basement at the end of the run and thus nearly full polymer expulsion from beneath the overburden sediments and limited the total depth of the subsidence.

Experiments with thicker initial substrate depths (η_{PI} = 16 cm) resulted in narrower basin widths when compared to those of thin initial substrate depth (η_{PI} = 8 cm) (Figure 1). Comparing the time series of width in the thin substrate runs (Figures 3C and 3D) with equivalent runs with thick substrates (Figures 4C and 4D), a greater finial width in thin initial substrate runs is observed. The initial thickness change in the experiment provided 8–10 cm differences in the final width between experiments with equivalent sediment supply conditions.

All experiments displayed two phases of basin width evolution as shown in Figures 3 and 4. Phase 1 was characterized by rapid basin widening once sedimentation initiated at

the start of the experiment. Phase 2 was the subsequent period of gradual basin widening that occurred somewhere approximately 5-15 minutes into the experimental run as growth of basin width was stabilized by increasing subsidence. Timing of the transition from initial rapid widening to subsequent slow widening of the basin was controlled by the rate at which sediments were supplied to the basin. Observing high sediment feed rate (4 cm^3/s) in Exp. 5, phase 1 of rapid basin widening was longer than that in Exp. 1, which had half the sediment feed rate (2 cm^3/s) (Figure 3C). In general, experiments conducted with high sediment inputs but 5-minute intermittency had smaller width profiles than experiments with 30-minute intermittency of the same sedimentation rate. Basin width evolution for experiments with rapidly pulsed sedimentation (5-minute intermittency), are very similar to width evolution of constant sediment input of half the sedimentation rate.

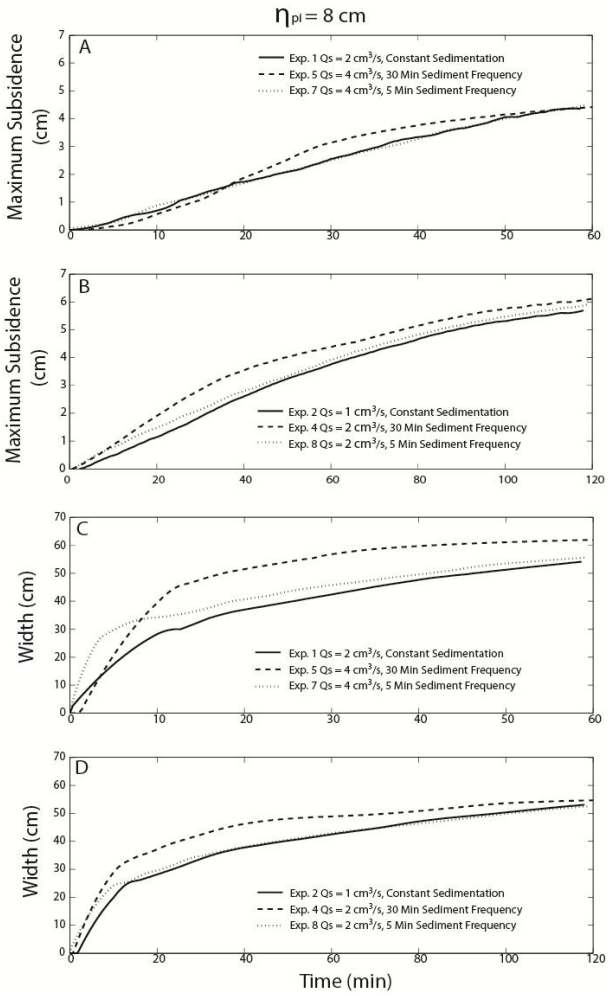

Figure 3: Measurements from experiments with 8 cm polymer substrate. (A) Subsidence development for Experiments 1, 5, and 7 measured at deposit centerline (maximum subsidence) – one hour experimental runtime. Exp. 1 received constant sedimentation for the length of the run while Exp.'s 5 and 7 received intermittent sedimentation of 30 and 5 minute intervals, respectively. (C) Basin width development corresponding to Experiments in (A). Note Exp. 5 displays a longer period of initial basin widening as well as greater final width profile when compared to Exp.'s 1 and 6. (B) Subsidence development for Experiments 2, 4, and 8 measured at deposit centerline (maximum subsidence) – two hour experimental runtime. Exp. 2 received constant sedimentation for the length of the run while Exp.'s 4 and 8 received intermittent sedimentation of 30 and 5 minute intervals, respectively. Note similar subsidence patterns in 30 min sediment frequency Exp. 5 (A) and Exp. 4 (B) – accelerating subsidence during sedimentation period followed by decelerating subsidence during corresponding intermittency periods. Exp. 4 undergoes two cycles of sedimentation that results in two subsidence accelerations and decelerations. (D) Basin width development corresponding to Experiments in (B).

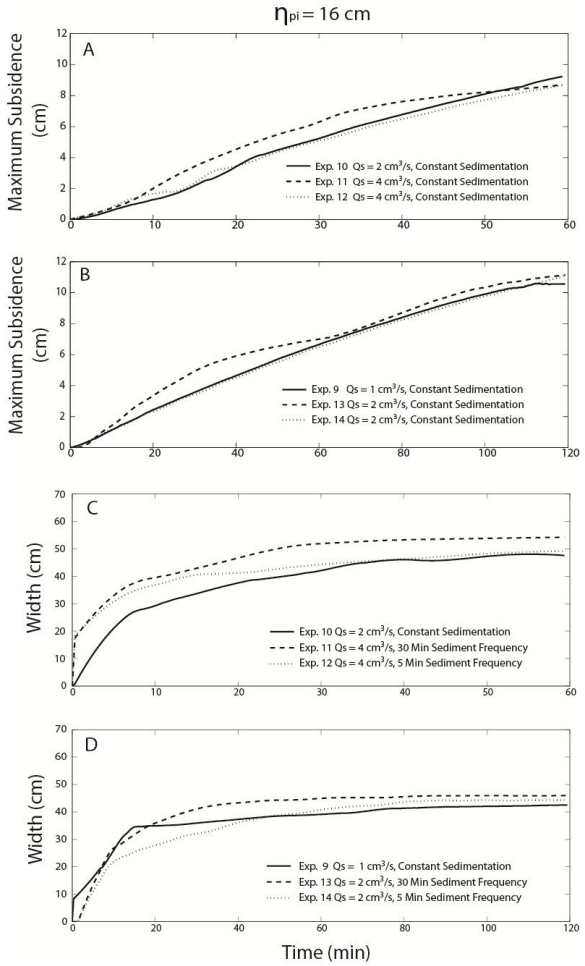

Figure 4: Measurements from experiments with 16cm polymer substrate. (A) Subsidence development for Experiments 10, 11, and 12 measured at deposit centerline (maximum subsidence) – one hour experimental runtime. Exp. 10 received constant sedimentation for the length of the run while Exp.'s 11 and 12 received intermittent sedimentation of 30 and 5 minute intervals, respectively. Note greater final subsidence in Exp.'s 10, 11, and 12 when compared to final subsidence observed in corresponding Exp.'s 1, 5, and 7 in Figure 1 A. (C) Basin width development corresponding to Experiments in (A). (B) Subsidence development for Experiments 9, 13, and 14 measured at deposit centerline (maximum subsidence) – two hour experimental runtime. Exp. 9 received constant sedimentation for the length of the run while Exp.'s 13 and 14 received intermittent sedimentation of 30 and 5 minute intervals, respectively. Note similar subsidence patterns in 30 min sediment frequency Exp. 11 (A) and Exp. 13 (B) – accelerating subsidence during sedimentation period followed by decelerating subsidence during corresponding intermittency periods. Exp. 13 undergoes two cycles of sedimentation that results in two subsidence accelerations and decelerations. (D) Basin width development corresponding to Experiments in (B). Note limited change in basin width throughout each of the runs in (D).

Role of Sedimentation Rate

The relationship between subsidence and applied sediment load (overburden thickness) was influenced by both the thickness of the salt body as well as the sediment accumulation rate (Figure 5). The highest amount of subsidence was achieved with lower sedimentation rates (Exp. 2 and 9 in Figure 5), while high sedimentation rate experiments (Exp. 5 and 11 in Figure 5) underwent considerably lower subsidence for the same overburden thickness. This response to sedimentation rate is exacerbated by the substrate thickness. As presented in the previous section, greater substrate thickness resulted in greater overall subsidence rate (compare Figures 3A and 3B with Figures 4A and 4B). As low and high sedimentation rates provided even greater discrepancy in amounts of subsidence in those conduced with thicker substrate (Figure 5B).

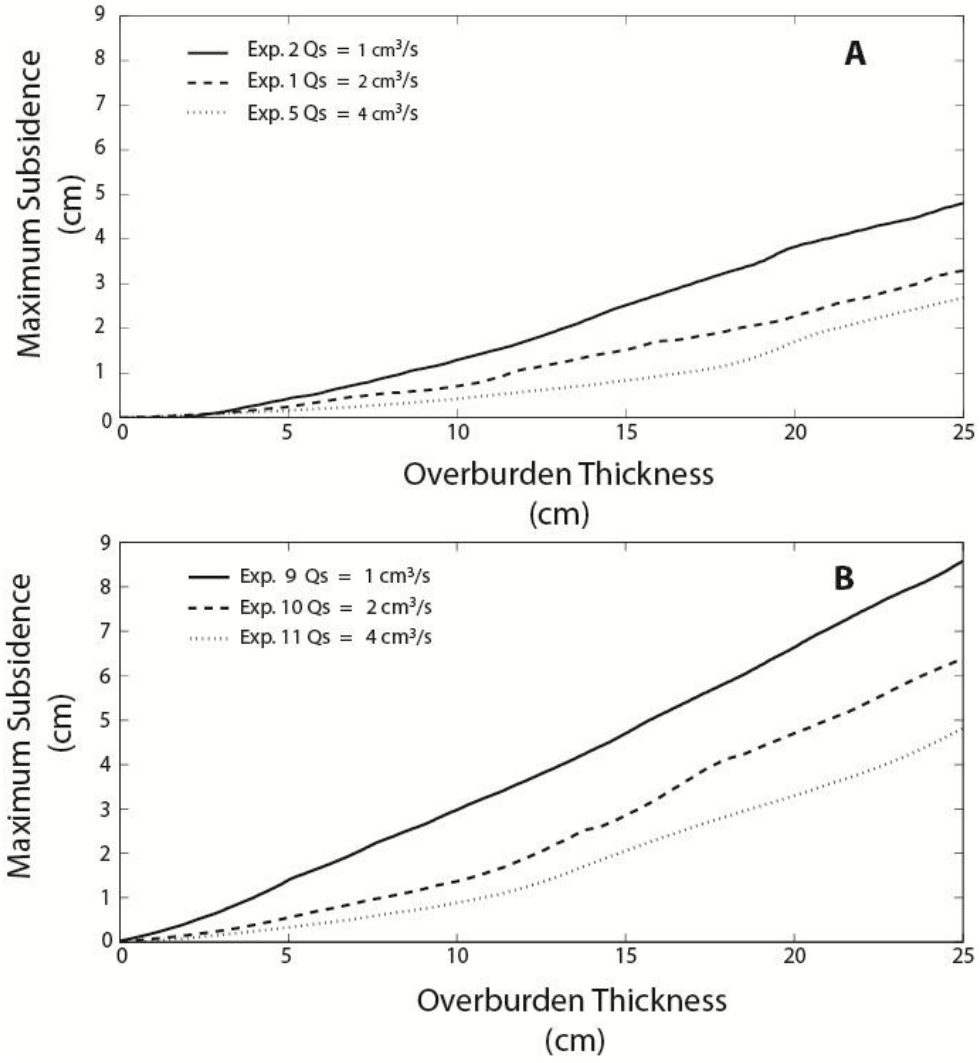

Figure 5: Non-linear relationship between overburden thickness and maximum subsidence. (A) Low, medium, and high sedimentation rates with 8 cm of polymer substrate. Note that Exp. 2 has the lowest sedimentation rate but displays the highest amount of subsidence. (B) Same low, medium, and high sedimentation rates as in (A) with 16 cm substrate thickness. Lowest sedimentation rate Exp. 9 displays the largest amount of subsidence. All Exp.'s with 16 cm substrate (B) undergo greater subsidence than their counterparts in (A).

Development of Non-linear Subsidence Patterns

In addition to substrate thickness and sedimentation rate, control of subsidence patterns were influenced by internal non-linearity due to increasing sediment load as sediments continue to enter the basin. Even with constant sediment supply rate in experimental runs, subsidence rate measured at the center of the deposit did not always increase linearly. Overburden thickness at the center of the deposit increases quickly during initial loading but gradually decreases due to lateral widening of the sediment pile. Subsidence rate increases quickly during the phase of rapid increase in overburden thickness but slows over time (Figures 6 and 7). After the initial loading phase in which overburden thickness rapidly increases, the subsidence rate stabilizes and starts to decrease even with the continuous increase in the thickness of sediment deposit at the center. This is thought to be driven both by lateral load spreading as mini-basin width increases as well as by frictional edge effects. Edge effects are hypothesized to result in restriction of polymer flow as accommodation space becomes restricted due to overburden sediments approaching the immobile substrate at the bottom of the experimental tank. Irregular subsidence rate was observed in runs with continuous sedimentation. These irregularities are likely results of both errors of image analysis as well as internal dynamics of the sediment pile responding to avalanching of sand down the sediment pile slope. The initial acceleration of the subsidence is greater in experiments with higher sedimentation rates (Figures 6 and 7).

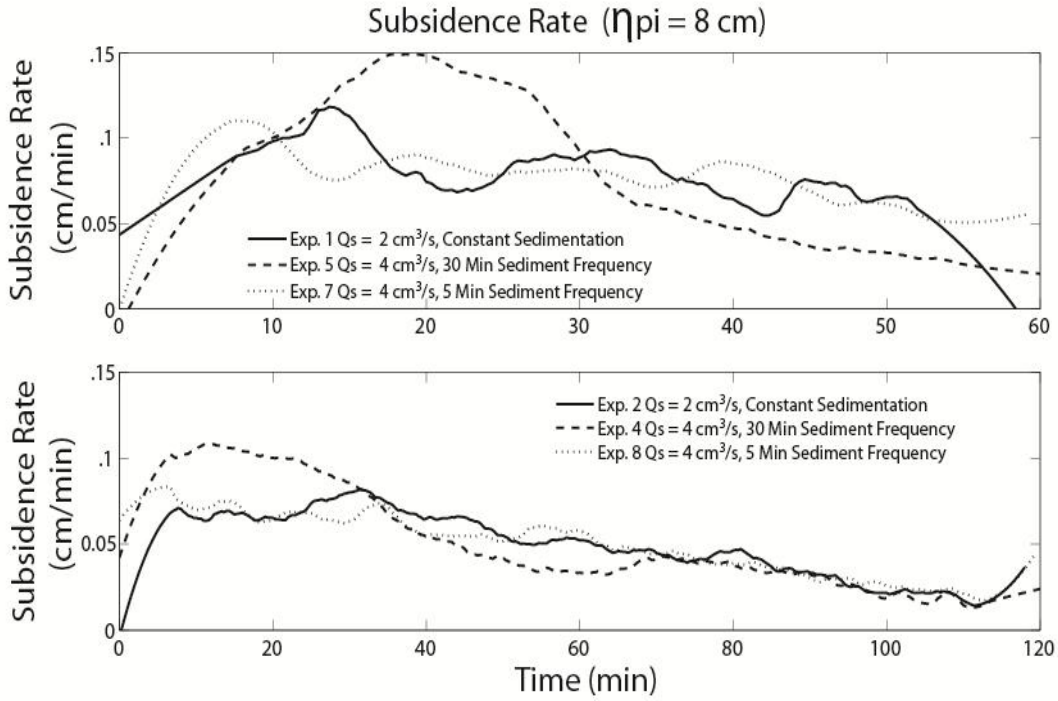

Figure 6: Subsidence rate through time for experiments with 8 cm initial substrate. Solid line represents continuous sedimentation experiments. Dashed line represents 30 minute sedimentation intermittency runs; dotted line represents 5 minute sediment intermittency runs. (A) Subsidence rate of Experiments 1, 5, and 7 measured at deposit centerline (maximum subsidence) – one hour experimental runtime. (B) Subsidence rate of Experiments 2, 4, and 8 measured at deposit centerline (maximum subsidence) – two hour experimental runtime. Subsidence response of individual sedimentation events is observed in experiments with intermittent sedimentation. Each cycle of sedimentation displays a corresponding acceleration and deceleration of the subsidence rate. These accelerations and decelerations have the largest magnitude during the initial cycle of sedimentation but a decrease in intensity through subsequent cycles. Over each experiment a gradual decrease in subsidence rate is observed throughout the run. Note subsidence rate for continuous sedimentation experiments is more consistent in runs lasting 2 hours as the basin subsides more steadily under lower sedimentation rates over longer timescales.

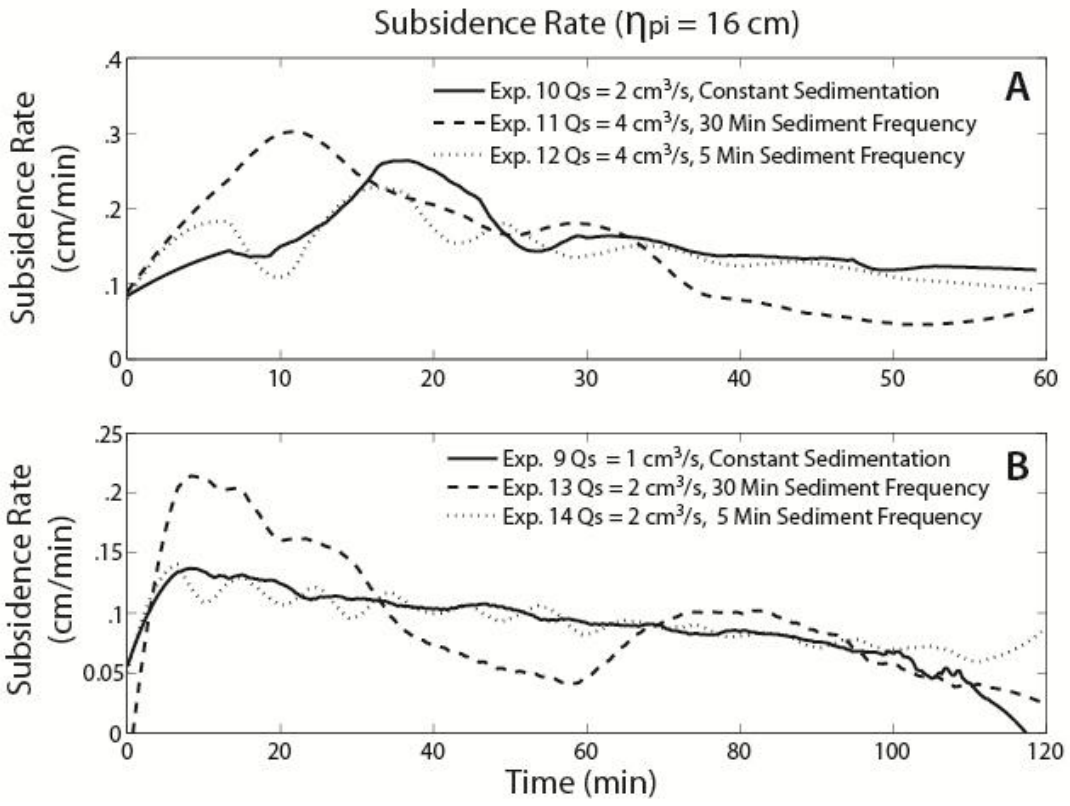

Figure 7: Subsidence rate through time for experiments with 16 cm initial substrate. Solid line represents continuous sedimentation experiments. Dashed line represents 30 minute sedimentation intermittency runs; dotted line represents 5 minute sediment intermittency runs. (A) Subsidence rate of Experiments 10, 11, and 12 measured at deposit centerline (maximum subsidence) – one hour experimental runtime. (B) Subsidence rate of Experiments 9, 13, and 14 measured at deposit centerline (maximum subsidence) – two hour experimental runtime. Higher subsidence rates are observed throughout runs with greater initial substrate thickness than for thin substrate thickness experiments. Irregular subsidence rate for continuous sedimentation likely results from both errors of image analysis as well as internal dynamics resulting from the pulsing of sediment pile slope. Note subsidence rate for continuous sedimentation experiments is more consistent in runs lasting 2 hours as the basin subsides more steadily under lower sedimentation rates over longer timescales. Note that over longer experimental runs (2 hour run) these irregularities are considerably less than in short (1 hour run) experiments indicating that these internal dynamics occur over short timescales and are less observable over long timescales.

Role of Sedimentation Frequency

Acceleration of subsidence was clearly observed in 30-minute intermittency experiments, (Exp.'s 5, 4, 11, and 13) (Figures 6 and 7). During periods of sedimentation an increase in the rate of subsidence was observed followed by a deceleration in subsidence when sedimentation stopped. Subsidence did not cease during paused sedimentation but the rate of subsidence decreased even with no change in the thickness of the sediment deposit. For example, Exp. 13 (Figure 4) displayed a clear acceleration and deceleration of subsidence over the first hour of experimental run. At runtime = 1 hour, the total subsidence of Exp. 13 (4 cm^3/s, 30-minute intermittency) and Exp. 9 (2 cm^3/s, continuous sedimentation) were approximately equal to each other as subsidence in Exp. 13 has decelerated a significant amount during paused sedimentation. Exp. 13 displayed a second period of accelerating subsidence during the second cycle of sedimentation that is less pronounced than those observed during the first hour of runtime (Figure 7B). The acceleration and decelerations of subsidence during pulsed sedimentation are also observed in 5-minute intermittency experiments. In these runs subsidence accelerations and decelerations are subtler than accelerations and deceleration of 30-minute intermittency experiments (Figures 6 and 7).

CHAPTER 4: DISCUSSION

The goal of the experiments was to evaluate the stratigraphy that results from subsidence of salt bodies due to loading of sediments. Experiments have revealed three important findings related to this problem. We first describe the linkage between sedimentalogical conditions and resulting subsidence patterns observed in experiments followed by a discussion of the stratigraphic patterns that result from these observed subsidence profiles as well as applications to field scale minibasins.

Substrate Thickness Control of Subsidence Patterns

Total vertical subsidence and basin width in experimental minibasins appeared to be dominantly controlled by the initial thickness of the polymer substrate (salt analogue). Experiments with thick (16 cm) substrate exhibited total subsidence approximately 40-50% greater than equivalent experiments with thin (8 cm) substrate. Greater subsidence in experiments with thicker substrate results from less friction from the basement on the flow of polymer from beneath the subsiding sediments.

As previously noted, thin substrate experiments were designed to simulate confined minibasin systems in which sediments are able to fully subside through the polymer substrate and contact the underlying rigid basement. In natural minibasin systems, the point of contact between overburden sediments and rigid basement is defined as a salt weld (Jackson and Cramez, 1989). Experiments with thick initial polymer thickness were defined as unconfined systems, in which no sediment welding was observed over the experimental run.

Due to the restriction of the ability of sediments to subside vertically, experiments with thin mobile substrate exhibited greater basin width than equivalent experiments of thicker polymer substrate. The sediment pile naturally maintains the sediment surface slope at the angle of repose and thus as vertical subsidence was restricted, sediments spread further laterally over equivalent time periods to experiments with thick initial substrate. In experiments of thick initial substrate the width of the basin remained constant once the equilibrium width profile was established. In these cases the subsidence was enough to accommodate the supplied sediment to maintain the equilibrium width of the basin. This resulted in nearly vertical walls of the minibasin that developed as a result of increased vertical subsidence of overburden sediments. This contrasted experiments with thin initial substrate in which minibasins continued to widen throughout the entire experimental run.

Effect of Sedimentation Rates and Patterns on Subsidence Patterns

In addition to control of subsidence patterns by initial substrate thickness, experimental results have illustrated dependence of subsidence on sedimentation rate. For minibasins of equivalent overburden thickness the basin receiving sediment at a lower rate will have undergone a greater amount of subsidence (Figure 5). Slower sedimentation rates results a slower increase in the sediment load results in a longer period of time for the substrate to respond to the applied load. This causes greater subsidence in basins receiving sediments slowly when compared to basins receiving sediments rapidly when the basins contain equivalent total volume of sediments.

A decrease in basin width was also observed to correspond with lower sedimentation rates (Figures 3 and 4). Because high vertical subsidence creates accommodation space in

low sedimentation rate experimental runs, basin width remains nearly constant throughout the experimental run once the basin width has been established (Figure 8). This is due to subsidence keeping pace with the growing thickness of the overburden sediments and created accommodation limiting the lateral spreading of the sediment.

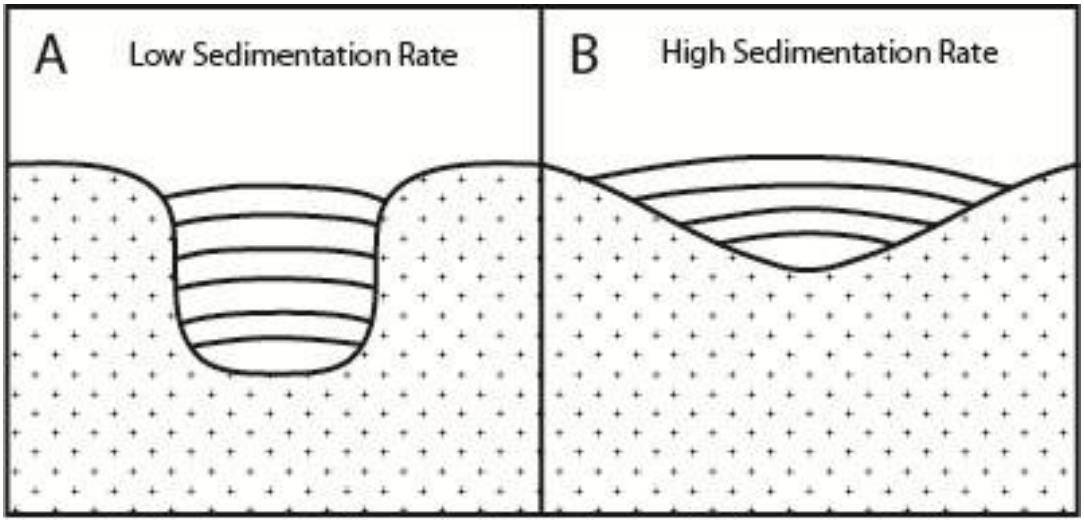

Figure 8: Cartoon illustration of mini-basin geometries developing under equivalent conditions but different sedimentation rates. (A) Developing mini-basin that has received sediment at a rate low enough for subsidence to keep up with overburden thickness. (B) Developing mini-basin in which sedimentation rate is outpacing subsidence rate resulting in lateral widening of the basin. Note vertical basin walls in (A) that correspond to higher created accommodation space within the basin for incoming sediments.

.

Effect of Internal Processes on Subsidence Patterns

Experiments were designed to investigate system responses to steady external forcing (i.e., constant sediment supply to the basin). Non-linear response observed in the subsidence profiles can be summarized in the followings. First, increasing weight of overburden sediments throughout basin development was observed to cause acceleration in the rate of subsidence. Second, decelerating subsidence rate was observed during periods of non-sedimentation.

Increase of subsidence rates occurred during phases of increasing sediment load. Even under the constant sediment supply, the sediment surface process changes the rate of increase in overburden thickness depending on the basin width changes. Accelerating subsidence is greatest as the minibasin initially begins to develop, as vertical aggradation of the sediment pile was most active. During continued growth of the basin, accelerations become muted due to lateral distribution of overburden loads as basin width becomes large. Increase of subsidence rate is observed most clearly during the initial period of basin development but is seen to become muted over time as the basin grows. We postulate that this decreasing subsidence rate is the result of increased frictional drag forces that act on the polymer as the sediment pile becomes large. Furthermore, frictional drag forces likely increase as the substrate underlying overburden sediments thins during continued subsidence, acting to decreasing the subsidence rate further. Experiments with intermittent sedimentation display the greatest amount of increase of subsidence rate during the initial pulse of sedimentation; subsequent sedimentation events have less acceleration of

subsidence rate. This illustrates the role minibasin width plays in the observed acceleration of subsidence as smaller basin widths are correlated to greater accelerations.

Deceleration of subsidence occurred during periods of non-sedimentation. Once sedimentation ceases a noticeable decrease in subsidence rate is observed (Figures 6 and 7). Withdrawn of salt underneath of the sediment allows the sinking of the deposit into the salt substrate. The decelerations are likely due to increase in the frictional effects acting on the interface between the substrate and the basement that retard the flow of polymer from beneath sediments as the substrate thickness gradually decreases even during the periods of intermittency. As with accelerating subsidence, these decelerations are most pronounced following the initial pulse of sedimentation. Subsequent cycles of sedimentation exhibit decelerations that are reduced in magnitude. This decrease in magnitude of deceleration is likely due to the suppressed acceleration prior to the decelerating stage. As the basin widens, the length over which friction force is acting also increases and thus diminishes the rate of subsidence. In addition to high frequency accelerations and decelerations of subsidence corresponding to each sedimentation event, all experiments exhibit an overall decrease in subsidence rate over the course of the experiment illustrating an increasing importance of frictional forces as the basin becomes large.

Theoretical Prediction of Subsidence Patterns

Experiments resulted in non-linear subsidence as a mobile substrate was loaded with sediments. Subsidence patterns were dependent on initial substrate thickness, sediment supply rate, and non-linear response of the substrate to changing sediment load. Here we

present a theoretical method to calculate these non-linear subsidence profiles. This calculation is useful method to capture experimental observations and apply to predictions of subsidence patterns in natural minibasins.

Polymer substrate used in experiments (SGM-36) as well as salt in sedimentary basins can be considered to behave as viscous Newtonian fluids when observed under strain rates resulting from sediment loading (Weijermars, 1986; Weijermars et. al, 1993). Strain rate $\dot{\gamma}$ may be related to applied stress τ in a Newtonian material by

1. $$\tau = \mu * \dot{\gamma}$$

where the constant of proportionality μ, represents the viscosity of the material. When observing a one-dimentional system the stress of the applied load of sediments can be described as

2. $$\tau = \frac{F}{A}$$

with F representing force over A area. Rearranging and simplifying yields:

3. $$\tau = \rho_c g \eta$$

Where ρ_c is the density of the overburden, g the acceleration due to gravity, and η the overburden thickness. Strain rate can be defined as

4. $$\dot{\gamma} = \frac{d}{dt}\left(\frac{\ell_o - \ell}{\ell_o}\right)$$

We define ℓ_o as the original substrate thickness, and ℓ as the deformed thickness. Using these relationships we can relate deformation D $\stackrel{\text{def}}{=} (\ell_o - \ell)$ over observation timestep Δt to overburden sediment load by

5. $$\frac{dD}{dt} = \rho g h \left(\frac{1}{\mu}\right) \ell_o$$

This formulation is a simple method to predict the subsidence rate resulting from an increasing sediment load. However, discrepancies between experimental and calculated subsidence patterns arise from two dimensional effects in experiments (Figure 9). Lateral load spreading of sediments acts to distributed the weight of the overburden and decreased the subsidence rate of the developing minibasin, additionally drag forces acting on the flow of substrate act to retard subsidence (Figure 9). To overcome this discrepancy in a simple way, the amount of deceleration of subsidence due to the distributed load can be empirically parameterized

6. $$\frac{dD}{dt} = \rho g h \left(\frac{1}{\mu}\right) \ell_o * \left(\frac{1}{k}\right)$$

where the term k represent subsidence deceleration predicted empirically from experimental data. This formulation for deformation predicts subsidence patterns that closely approximate experimental subsidence patterns that developed under equivalent sedimentary conditions (Figure 8).

Equation 6 provides a method for approximation of the subsidence patterns of a field scale minibasin. To apply equation 6 to the field scale knowledge of the age of the minibasin as well as minibasin geometry are required to provide an accurate approximation of the subsidence history. Ideally age control throughout the basin would provide an incomplete record of subsidence that could be interpolated using equation 6.

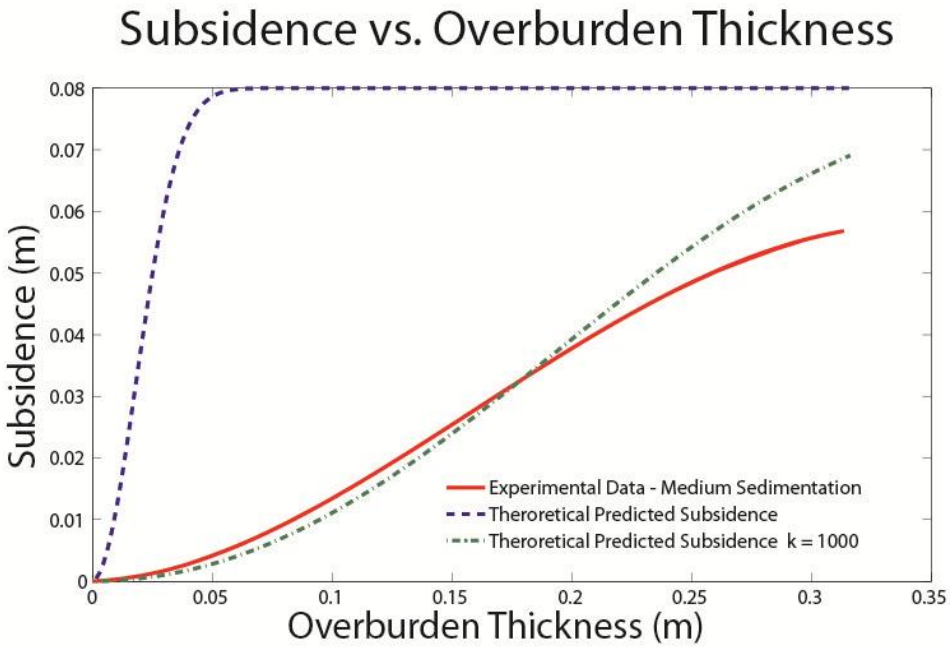

Figure 9: Comparison of experimental subsidence data from Exp. 2 (2hr constant sedimentation of 2 cm^3/s with 8 cm initial substrate thickness)-(solid line) with theoretically calculated subsidence of equivalent conditions-(dashed line). Subsidence predicted from theoretical calculation is much greater than that observed in experiments due to resisting frictional drag forces that act to retard the flow of polymer. Using an empirical correction term (k) to account for these effects a much closer approximation of the subsidence profile is developed-(green dotted dashed line).

Scaling Experimental to Field Scale Minibasins

Application of experimental results to field scales necessitates comparison of the time scales of each system. We take the scaling approaches of deforming salt experiments outlined in Weijermars et al. (1993). Non-dimensional time t^* can be accomplished by:

7. $$t^* = \frac{t\rho_c g\eta}{\mu}$$

where μ represents viscosity, g denotes gravity, and ρ_c denotes density of overburden, and η denotes overburden thickness, subscript c indicates properties of the overburden. With both natural and experimental systems under the uniform gravity the previous equation can be used to scale experimental time and to compare with natural minibasin time scale as

8. $$t_{pro} = \left(\frac{\mu_{pro}\,\rho_{mod}\eta_{pro}}{\mu_{mod}\rho_{pro}\,\eta_{mod}}\right) t_{mod},$$

where the subscript mod (model) represents experimental systems and the subscript pro (prototype) represents the natural (field scale) system. Using equation (8) comparison of the time scales of experimental and natural systems can be accomplished. Experiments were conducted over time periods of 1 – 2 hours with average overburden thicknesses of 0.35 m. When compared to a Pleistocene Gulf of Mexico minibasin with an overburden thickness of several 100 m (Beaubouef, 2003) and average underlying salt viscosity of 10^{17} Pa s (Weijermars et al., 1993), the total experimental runtime for a 1-hour experiment can be calculated to have captured approximately 125 ka of evolution of a the field scale system. A 2-hour experimental runtime represents approximately 250 ka of natural minibasin

evolution. Although the current experiments may not capture full minibasin evolution over a few million years, a significant portion of basin stratigraphy still can be comparable to the experimental results. For a minibasin subsiding at rates of up to 1 km/ma (Hudec 2009), experiments capture evolution of stratigraphic sequences up to ~100-m thick depending on sedimentation rates in natural systems.

Stratigraphic Implications: Modeling Approach

In experiments, depositional processes were controlled but stratigraphic surfaces within the sediments were difficult to identify due to the homogeneity of the supplied sediment. Contrastingly, in field scale minibasins stratigraphic surfaces are imaged but depositional processes relating to their development must be inferred. To provide a better linkage between stratigraphy and their developmental process, a simple stratigraphic model was developed using the subsidence patterns observed in experiments. The model is two-dimensional and sediment inputs (q_t) must be converted under a specified sediment surface geometry (Figure 9A). We assume that the sediment surface maintains a constant slope over time. In fact, sediment pile in the experiments kept slopes to both sides at the angle of repose. Using geometries that mimic those observed in experiments, the maximum thickness of the sediment above the initial substrate top elevation η_T overburden at the center of the basin can be predicted as

9. $$\eta_T = \frac{1}{2} L * S_t$$

where S_t represents sediment surface slope and L denotes the minibasin width. For a basin receiving sediment at a known flux q_t

10. $$\frac{1}{2}\eta_T * L = q_t * t - A_b,$$

where A_b represents the area of minibasin deposit that has subsided into the substrate (Figure 2). Combining (9) and (10) to solve for sediment thickness η_T yields

11. $$\eta_T = \sqrt{S_t(q_T t - A_b)}$$

In the model, we use an empirical relationship between the total overburden thickness (η_T + η_B) and subsidence rate that were both observed from the experiment and apply to the model (Figure 10B). The process of calculation of subsidence rate as a function of overburden thickness is repeated as the substrate is loaded with sediments. The model creates synthetic stratigraphy that develops purely as a response to loading induced subsidence. The total number of stratigraphic time horizons plotted can be specified by the user. Although using simple geometrical rules, this model gives insight into the stratigraphic patterns that are caused by internal system dynamics, i.e. subsidence patterns, independent of changes to external forces. Figure (11) displays synthetic stratigraphy from several different model results of different scenarios of sedimentation and subsidence patterns as well as corresponding experimentally derived patterns. Modeled subsidence and basin width profile evolution closely resembles that of experimental results indicating that the stratigraphic model honors experimentally derived data (Figure 11).

The stratigraphic model presented here provides a close approximation to the results observed in experiments but it does have several shortcomings. First, upwelling of salt

adjacent to the developing minibasin is not modeled using this method, as substrate deformation is modeled as a function of overburden thickness. Flow dynamics that would result in upwelling are not captured. While this might lead to slightly unrealistic minibasin geometries, this problem is mitigated by the subsidence profiles that are used in the model. Utilizing subsidence profile is derived from experimental data within the model incorporates the effects of salt stock rise. Because the process of upwelling salt occurs in experiments, subsidence data derived from each experiment captures the effect that this process has on these subsidence profiles. Second, modeled results only account for simple minibasin geometry similar to the point-sourced basin of the experiments.

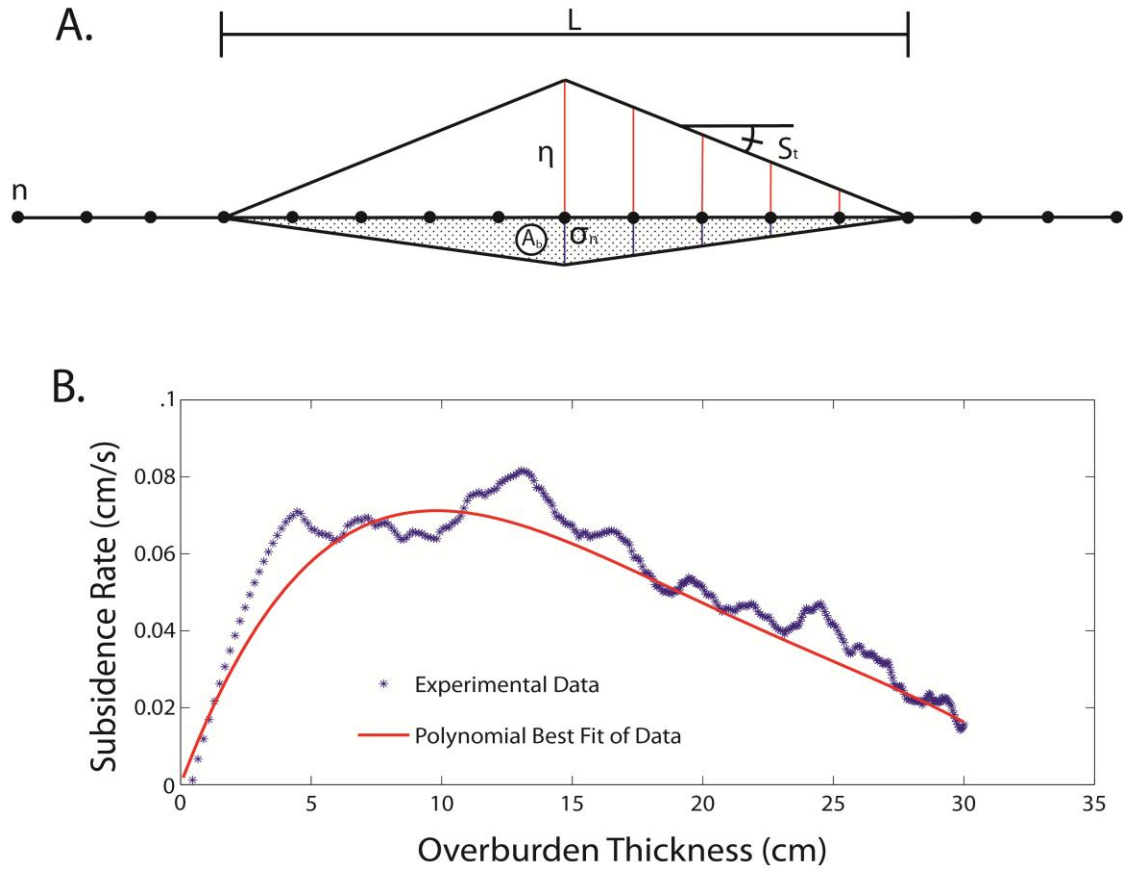

Figure 10: (A) Schematic of the setup of synthetic stratigraphic model based on conservation of area. For specified sediment feed rate q_s, the overburden thickness η at each model node n can be calculated. With St representing the angle of repose of sediments, σ deformation due to sediment load, A_b the total area of created accommodation, and L basin width. (B) Relationship between overburden thickness and subsidence rate derived from experiments. Experimental data is displayed as (*), best fit 4th order polynomial is displayed as a solid line. Using this relationship subsidence at each model node n can be calculated once the overburden thickness η is known. This process is repeated for each model node at each model time step to develop synthetic stratigraphy which undergoes deformation due to continued subsidence.

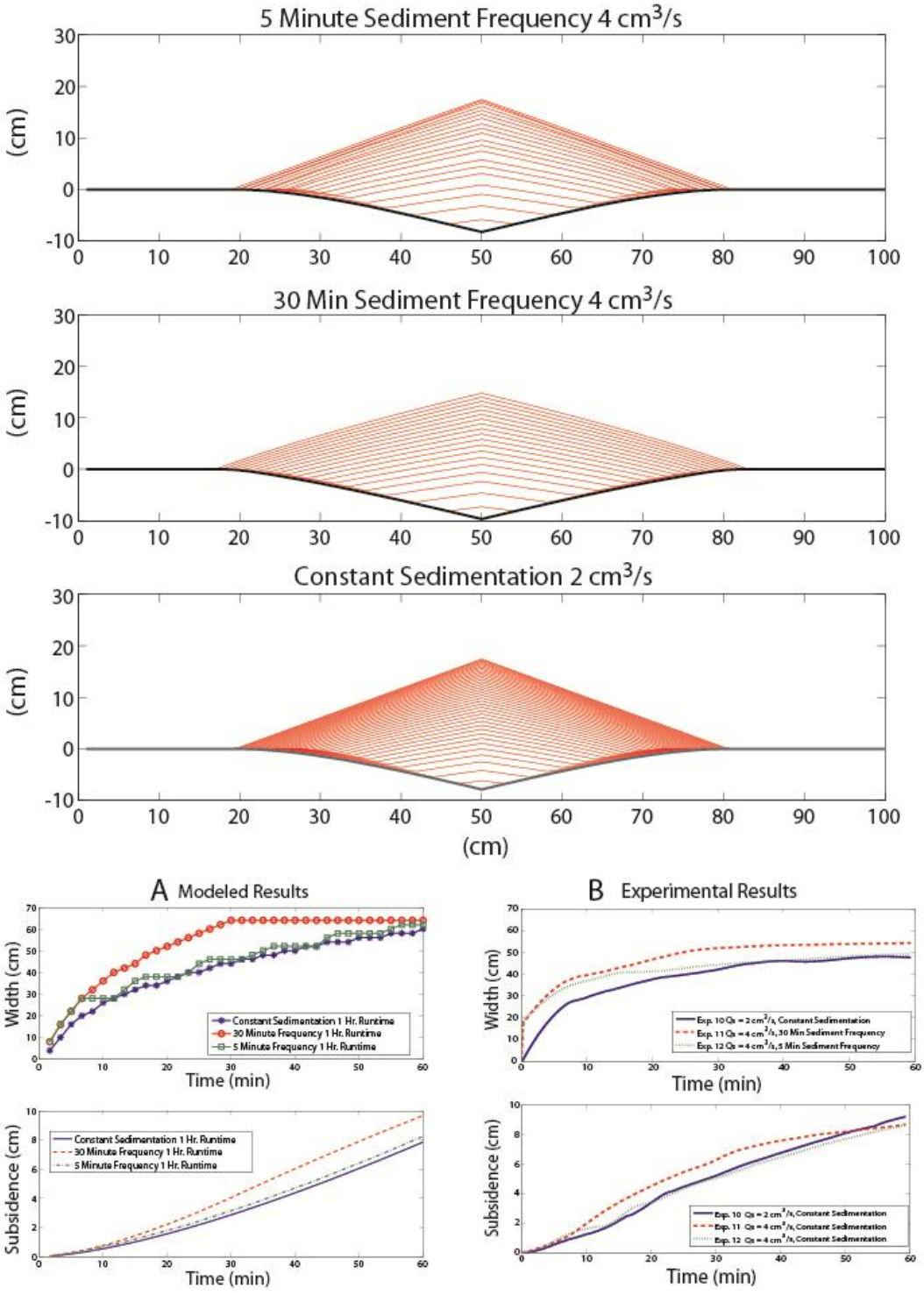

Figure 11: Caption on following page.

Figure 11: Model results simulating equivalent conditions to experiments 10, 11, and 12 with 5 min sediment frequency (Exp. 12), 30 min sediment frequency (Exp. 11) and constant sedimentation (Exp. 10). Red lines represent stratigraphic timelines of overburden sediment surface every 0.6 minutes. Bottom panels (A) and (B) compare modeled basin width and subsidence results with experimentally derived data. A close resemblance between the model and experimental results was observed in both basin width and subsidence evolution, indicating that the stratigraphic model honors experimental results.

Development of Minibasin Stratigraphy

The Brazos-Trinity Intra-Slope System is series of linked intra-slope minibasins that have been well imaged and studied with modern 2D and 3D seismic imaging, as well as several borehole core studies (Winker 1996; Beaubouef and Friedmann, 2000; Prather et al., 2012; Primez et al., 2012). This system is an excellent natural analogue for modeled systems as it has been a location of high subsidence and sedimentation over the past 100 ka (Primez, 2012). Additionally, it represents a modern to recent analogue for ancient deep-water depositional systems which are frequently the target of hydrocarbon exploration (Primez et al., 2012). Early studies of these basins have interpreted sedimentary deposits to have evolved under static accommodation space (Beaubouef and Friedmann, 2000). Their depositional model describes basin evolution as a three stage process, 1) a ponded fill phase of an underfilled basin (Figure 12-1A 1B), 2) a perched filling stage as basin accommodation space becomes limited (Figure 12–1B and 1C), and 3) a bypassing phase once the basin has become overfilled (Figure 12-1C). This fill-and-spill depositional sequence of filling of accommodation space and subsequent bypass of sediments has been described in Prather et al. (1998) and others. Although, this interpretation of basin filling provides an accurate description of stratigraphic architecture at present static conditions, it does not fully incorporate the influence of sedimentary processes within a syn-depositionally subsiding basin. Experimental and model results from this study have illustrated the role changing sediment load have on basin subsidence profile and consequent accommodation space. Using these findings we propose that minibasin depositional models can be improved in two ways: 1) Minibasins systems evolve in response to a dynamic

relationship between subsidence rate and sedimentation rate (Figure 12-2). 2) During sea-level lowstand, sedimentation rate far outpaces subsidence rate due to the influx of shelf edge sediments (Pirmez et al., 2012). Because of this the majority of subsidence occurs during periods of low deposition rates that are often associated with sea-level highstand (Pirmez et al., 2012).

Experimental results suggest that subsidence rates are sensitive to the rate of sedimentation within the minibasin (Figure 5). Experiments have shown that for constant volumes of sediment, basins with a lower sedimentation rate realize a greater amount of subsidence. This suggests that amount of accommodation space within a minibasin is highly dependent on the relationship between sedimentation rate and subsidence rate. For a basin receiving sediment at a low rate, basin subsidence will proceed at a faster pace than accommodation space is filled. This model of minibasin development suggests that during periods of low sedimentation, subsidence will outpace sediment accumulation resulting in the development of ponded stratigraphic architectures (Figure 12- 2B). For increased sedimentation rates the subsidence of the basin cannot keep pace with the rate at which sediments accumulate and the accommodation space within the basin becomes infilled (Figure 12 -2C). As the basin gradually thickens, the substrate thickness decreases, which would also cause a decrease of subsidence rate. This dynamic evolution of minibasin subsidence in response to changing loading rates is a time dependent process. In order for significant accommodation space to develop low sedimentation and/or low frequency of sedimentation must occur for a period of time long enough for the basin to subside in response to the sediment load. If low sedimentation occurs for only a short period of time

subsidence will only briefly outpace sediment accumulation and significant accommodation space within the basin will not develop.

Experimental results have provided an additional mechanism for the development of perched stratigraphic architectures within minibasins. Throughout experimental runs a gradual deceleration in subsidence rate was observed as the minibasin developed (Figures 6 and 7). This deceleration was due to increasing load spreading as the minibasin widened as well as frictional edge effects due to decreasing substrate thickness caused by subsidence. It is inferred that this same subsidence deceleration will autogenically occur in natural minibasins as salt is dispelled beneath the overburden sediments. Over time the decrease in salt thickness beneath the basin will cause a decrease in the subsidence rate of the basin and accommodation space will become limited regardless of sedimentation rates.

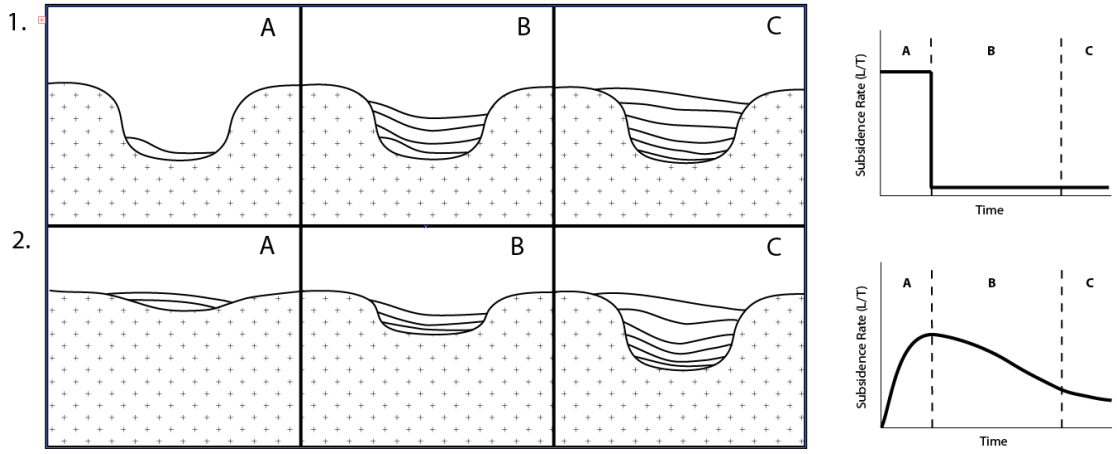

Figure 12: Two models of minibasin evolution. Sequence 1 represents high initial subsidence that creates accommodation space within the basin. During time 1A basin accommodation is created through rapid subsidence. Following this period of rapid subsidence decreased subsidence results in filling of basin accommodation through continued sedimentation (1B). By time period 1C accommodation space has become limited and sediments are beginning to spill out of the basin resulting in perched stratigraphic packages. Sequence 2 represents a basin evolving dynamically in response to changing sediment load. 2A represents a model with low initial accommodation; space is created in response to the applied sediment load similarly to observed in experimental results. In this model stratal geometries are governed by the relationship between sedimentation rate and subsidence rate. Low sedimentation rate results in subsidence that is greater than how quickly sediments accumulate. This results in periods where sediments are able to pond within accommodation space (2B). If sedimentation increases subsidence can no longer keep pace with the accumulation of sediments and accommodation space begins to become infilled (2C). If rapid sedimentation occurs long enough accommodation within the basin will be completely infilled and sediments will begin to overspill the basin.

CHAPTER 5: CONCLUSIONS

Conclusions

1. A series of experiments were conducted to explore the response of differential sediment loading on minibasin subsidence patterns. Experimental results have shown that subsidence patterns due to differential loading within salt withdrawn minibasins are dependent on 1) initial substrate thickness (salt body thickness), 2) sediment supply rate to the basin, and 3) accelerations and decelerations in subsidence rate as the substrate responds to changing loading conditions. Understanding the control of these variables on subsidence patterns has allowed a theoretical calculation of subsidence patterns under a wide range of conditions. Sedimentation rate was observed to be a controlling factor in the width evolution of minibasins. Low sedimentation rates were observed to develop narrower basins with steeper basin walls than basins that evolved under equivalent conditions but higher sedimentation rates.
2. Effect of variable subsidence on stratigraphy was observed utilizing a stratigraphic model that created synthetic stratigraphy that was deformed by ongoing subsidence. This computational model creates synthetic stratigraphic timelines that can illustrate how variable subsidence due to an increasing sediment load causes deformation of overburden sediments. Model results closely resemble those observed in experiments.
3. Experimental results have illustrated that stratigraphic patterns are highly dependent on the response of salt substrate to sediment supply rate. Relatively low sediment

supply rates can result in subsidence rates that are greater than overburden sediments thicken. This drives an increase in accommodation within the basin as space is created faster than it is filled. Contrastingly relatively high sediment supply rates have been observed to result in thickening of the overburden sediments at rates greater than the sediments will subside into the substrate resulting in decreased accommodation within the minibasin. Based on experimental results we propose a new model of minibasin development that incorporates the dynamic evolution of minibasins as they respond to sediment loading. This model is incorporates the observations that subsidence patterns within these basins are a function of sediment supply rates. In this model accommodation within the basin is created concurrently with sediment loading. Initially basin accommodation is low and an initial load of sediment acts to initiate subsidence. As the basin continues to develop low sedimentation rates will produce subsidence rates that are greater than overburden sediments thicken, resulting in increasing basin accommodation and ponding of sediments within the basin. However, should sedimentation rates increase, sediment accumulations will proceed at a faster pace than accommodation space increases, resulting in an overall decrease in accommodation within the basin. If high sedimentation rates continue for an extended period of time accommodation within the basin will become completely filled and overspill of sediments will occur.

Appendix: Stratigraphic Modeling Code

The following code was written in MATLAB 7.10 by the author to model synthetic stratigraphy that developed in response to deformation of a mobile substrate. The code utilizes the subsidence rate data derived from experiments to predict subsidence based on overburden thickness. The 2-Dimentional conservation of area model utilizes area of inputted sediments to predict the stratigraphic timelines as they evolve over time. This geometrical relationship is governed by Equations 7, 8, and 9 presented above.

```
%% This program creates a synthetic stratigraphy based on subsidence
%% patterns observed in experiments.
%% Author Bryant Kopriva 4/30/2012

clear all

%% These parameters must be updated for each experimental run
St = .1; % Angle of repose of sand
Qs = .001; % Sediment feed rate (L/S)
t_step = 100; %Timestep (s)
N_step = .01; % Gridstep (m)
t = 2;  % Runtime hours
int = 30; % Intermittency (min)
Srate = [-5.3*10^-10,4.65*10^-7,-.00015,.018,0]; %Subsidence rate as a
function of thickness

time_s = t * 3600; % Runtime seconds
steps = time_s / t_step; % Number of timesteps
steps = round(steps);
int = int * 60;
period = int * 2;
space = period / 2 /t_step;

%Set up sediment input function
Q = ones(1,steps);
for k = 1 : steps
    Tnew(k) = t_step * k;
    if mod(Tnew(k),period) == (int+t_step)
       Q(k:k+space-1) = 0;
    end
end


% Calculate area per second using feed rate and 10cm thick flume
A_sec = 1 / Qs; %%Seconds per liter
A_cm = 400 / A_sec; %% CM^2 per second
A_m = A_cm *10^-4; %% M^2 per second
A_m = Q.*A_m;
```

```
%% Boundary Conditions.
Area = A_m(1) * t_step;
L = sqrt((Area/St));
Eta_m = (St*L)/2;
A_sub = 0; % Area of subsidence.

% Define grid space.
Eta = zeros((1/N_step), steps);
SubSum = zeros((1/N_step), steps);
Thick = zeros((1/N_step), steps);

% Initial sediment surface profile (Step 1)
Eta(50,1) = Eta_m;
for k = 1 : 49
    G_step = N_step * k;
    Eta_new(k) = Eta_m - (St * G_step);
    if Eta_new(k) <= 0
        Eta_new(k) = 0;
    end
     Eta(50+k,1) = Eta_new(k);
     Eta(50-k,1) = Eta_new(k);
end

%% Apply polynomial to Eta to find subsidence (Main Loop).

for j = 1 : steps
    time(j) = t_step * j /60; %Time in minutes.

    % Calculate total sediment area at timestep j.
    A_t(j) = sum(A_m(1:j))*100;

    % Calculate total sediment thickness.
    for k = 1 : 100
        Thick(k,j) = Eta(k,j) + SubSum(k,j);
    end

    Thick_max(j) =  Thick(50,j);

    % Caculate Subsidence (Step 2).
    %first we use thickness to get the subsidence rate.
    for k = 1 : 100
         S(k,j) = polyval(Srate,(Thick(k,j)))*10^-2;
    end

    %Now we get subsidence for the timestep by multiplying the subsidence
    %rate by the time interval.
    Sub(:,j) = S(:,j)*t_step;

    %We get the total current subsidence by summing up the previous times
    %step's subsidence.
```

```
    for k = 1 : 100
        SubSum(k,j)= sum(Sub(k,:),2);
    end


     % Calculate area of accommodation space  (multiply by 10^-2
     % because grid(x) is in cm space).
     A_sub(j) = sum(SubSum(:,j))* 10^-2;

    % Update Eta Max with continued sediment input.
    Eta_m(j+1) = sqrt(St*(A_t(j) - A_sub(j)));

    % Update Eta Profile.
    Eta(50,j+1) = Eta_m(j+1);
    for k = 1 : 49
    G_step = N_step * k;
    Eta_new(k) = Eta_m(j+1) - (St * G_step);
    if Eta_new(k) <= 0
        Eta_new(k) = 0;
    end
     Eta(50+k,j+1) = Eta_new(k);
     Eta(50-k,j+1) = Eta_new(k);
    end

   % Exclude Eta profile when sedimentation is = 0.
   if j > 1
      if  Q(j-1) == 0, Q(j) == 0
       Eta(:,j) = NaN;
      end
   end

    % Find the width and depth of the basin at each timestep.
    y1(j) = find(SubSum(:,j),1,'first');
     if y1(j) == 1
         y1(j) = NaN;
     end
     y2(j) = find(SubSum(:,j),1,'last');
     if y2(j) == 100
         y2(j) = NaN;
     end
     width(j) = y2(j) - y1(j);
     MaxSub(j) = SubSum(50,j)*100;
end

% Transform Subsidence to negative values for plotting.
Sub_neg = SubSum*-1;

% Update previous Eta Profiles by subtracting subsidence.
    for k = 1:j
        A(k) = A_t(k)/2;
        As(k) = A_sub(k)/2;
```

```
    B(k) = 2*(A(k)-As(k))/(Eta(50,k)-Sub(50,k));
    for s = 1 : 100
    Eta(s,k) = Eta(s,k) - SubSum(s,j-(k-1));
    end
end
```

Glossary

Confined System:	Experiment does form salt weld by end of experimental run
Unconfined System:	Experiment does not form salt weld by end of experimental run
A:	Area
A_b:	Area of created accommodation space
D:	Vertical deformation (analogous to η_b)
F:	Force
g:	Gravity
L:	Minibasin width
l:	Final length
l_o:	Initial length
k:	Empirical constant of subsidence (derived experimentally)
q_s:	Sediment flux
S_t:	Overburden topset slope
t:	Time
t*:	Dimensionless time
$\dot{\gamma}$:	Strain rate
μ:	Viscosity of substrate
η:	Total thickness of overburden sediments (η_T +η_b)
η_b:	Vertical subsidence (displacement)
η_T:	Overburden sediment thickness above original salt surface
η_{PI}:	Initial substrate thickness

τ:	Normal stress
Subscript (mod):	Model (experimental) parameters
Subscript (pro):	Prototype (natural system) parameters

References

Beaubouef, R., & Friedmann, S. (2000, December). High resolution Seismic/sequence stratigraphic framework for the evolution of pleistocene intra slope basins, western Gulf of Mexico: depositional models and reservoir analogs. *GCSSEPM Foundation 20th Annual Research Conference Deep-Water Reserviors of the World*.

Cohen, H., & Hardy, S. (1996). Numerical modelling of stratal architectures resulting from differential loading of a mobile substrate. *in Alsop, G. I., Blundell, D. J., and Davison, I., eds., Salt Tectonics, Geological Society, London, Special Publications, 100*, 265-273.

Hudec, M. R., Jackson, M. P., & Schultz-Ela, D. D. (2009, January/February). The paradox of minibasin subsidence into salt: Clues to the evolution of crustal basins. *GSA Bulletin, 121*(1/2), 201-221.

Humphris, C., Jr. (1979). Salt movement in continental slope, northern Gulf of Mexico. *AAPG Bulletin, 63*, 782-798.

Jackson, M., & Cramez, C. (1989). Seismic recognition of salt welds in salt tectonics regimes (ext. abs.), in Gulf of Mexico salt tectonics, associated processes and exploration potential. *Society of Economic Paleontologists and Mineralogists, Gulf Coast Section, 10th Annual Research Conference Program and Extended and Illustrated Abstracts*, 66-71.

Jackson, M., & Talbot, C. (1991). A glossary of salt tectonics. *The University of Texas at Austin, Bureau of Economic Geology Circlular, 91*(4), 44 p.

Jackson, M. P., & Talbot, C. J. (1994). Regional extension as a geological trigger for diapirism . *GSA Bulletin, 106*, 57-73.

Lamb, M. P., McElroy, B., Kopriva, B., Shaw, J., & Mohrig, D. (2010, September/October). Linking river-flood dynamics to hyperpycnal-plume deposits: Experiments, theory, and geological implications. *GSA Bulletin, 122*(9), 1389-1400.

Madof, A. S., Christie-Blick, N., & Anders, M. H. (2009, April). Stratigraphic controls on a salt-withdrawl intraslope minibasin, north-central Green Caynon, Gulf of Mexico. *AAPG Bulletin, 93*(4), 535-561.

Normark, W., Posamentier, H., & Mutti, E. (1993). Turbidite systems: State of the art and future directions. *Reviews of Geophysics, 31*, 91-116.

Pirmez, C., Prather, B. E., Mallarino, G., O'Hayer, W. W., Droxler, A. W., & Winker, C. D. (2012). Chronostratigraphy of the Brazos-Trinity depositional system, western Gulf of Mexico: Implications for deepwater depositional models. *Application of the Principles of Seismic Geomorphology to Continental-Slope and Base-of-Slope Systems: Case Studies from Seafloor and Near-Seafloor Analogues SEPM Special Publication , 99*, 111-143.

Prather, B., Booth, J., Steffens, G., & Craig, P. (1998, May). Classification, Lithologic Calibration, and Stratigraphic Succession of Seismic Facies of Intraslope Basins, Deep-Water Gulf of Mexico. *AAPG Bulletin, 82*(5A), 701-728.

Prather, B. E., Pirmez, C., & Winker, C. D. (2012). Stratigraphy of linked intraslope basins: Brazos-Trinity system western Gulf of Mexico. *Application of the Principles of Seismic Geomorphology to Continental-Slope and Base-of-Slope Systems: Case Studies from Seafloor and Near-Seafloor Analogues, SEPM Special Publication , 99*, 83-109.

Schultz-Ela, D., & Jackson, M. (1995). Relation of subsalt structures to suprasalt structures during extension. *AAPG Bulletin, 80*, 1896-1924.

Talbot, C. J. (n.d.). Extrusions of Hormuz salt in Iran. *Geological Society of London Special Publication, 143*, 315-334.

Vendeville, B., Ge, H., & Jackson, M. (1995). Scale models of salt tectonics during basement-involved extension. *Petroleum Geoscience, 1*, 179-183.

Vendeville, B., & Jackson, M. (1992). The fall of diapirs during thin-skinned extention. *Marine and Petroleum Geology , 9*, 354-371.

Vendeville, B., & Jackson, M. (1992). The rise of diapirs during thin-skinned extention. *Marine and Petroleum Geology, 9*, 354-371.

Vendeville, B. C., Ge, H., & Jackson, M. P. (1995). Scale models of salt tectonics during basement-involved extension. *Petroleum Geoscience, 1*, 179-183.

Weijermars, R. (1986). Finite strain of laminar flows can be visualized in SGM36-polymer . *Naturwissenschaften , 73*(1), 33-34.

Weijermars, R., Jackson, M., & Vendeville, B. (1993). Rheological and tectonic modeling of salt provinces. *Tectonophysics, 217*, 143-174.

Winker, C. D. (1996). High-resolution seismic stratigraphy of a Late Pleistocene submarine fan ponded by salt-withdrawn mini-basins on the Gulf of Mexico continental slope. *Offshore Technology Conference, Proceedings, 8024*, 619-628.

Winker, C. D., & Booth, J. R. (2000, December). Sedimentary Dynamics of the Salt-Dominated Continental Slope, Gulf of Mexico: Integration of Observations from the Seafloor, Near-Surface, and Deep Subsurface. *Deep-Water Reservoirs of the World: 20th Annual, 15*, 1059-1086. doi:10.5724/gcs.00.15.1059

Vita

Bryant Timothy Kopriva was born in Springfield, Missouri and grew up in Hurst, Texas. After graduating from Laurence D. Bell High School he enrolled in the University of Texas at Austin. He graduated with a Bachelor of Science degree in May 2010. In August 2010 he entered the Graduate program in the Jackson School of Geosciences at the University of Texas at Austin. Bryant's research interests include sedimentary processes, sequence stratigraphy and carbonate depositional systems. Upon completion of his degree Bryant will begin work at XTO Energy (now ExxonMobil) in Fort Worth, Texas.

Permanent address: 1012 Calloway Dr.
Hurst, TX 76053
bryant.kopriva@gmail.com

This thesis was typed by the author.